Thermochimica Acta, 113 (1987) 331–339
Elsevier Science Publishers B.V., Amsterdam – Printed in The Netherlands

CALORIMETRY OF THE HYDRATION OF CALCIUM ALUMINATES WITH VARIOUS GLASS CONTENTS

THOMAS P. ZGAMBO

The Gillette Company, Boston, MA 02106 (U.S.A.)

JOSEPH G. GRIFFIN * and KENNETH E. DAUGHERTY **

Department of Chemistry, North Texas State University, Denton, TX 76203 (U.S.A.)

MENASHI D. COHEN

Department of Civil Engineering, Northeastern University, Boston, MA 02115 (U.S.A.)

(Received 18 August 1986)

ABSTRACT

The following series of high-purity calcium aluminates was synthesized and characterized: CA, CA_2, C_3A, $C_{12}A_7$, C_3A_2M, and $C_6A_4M\bar{S}$. The compounds were prepared with varied glass content, determined by powder XRD, microscopy and IR spectroscopy. Each compound was hydrated adiabatically for 24 h at 25°C. Heat evolution measurements were conducted concurrently with hydration, and thermogravimetric measurements were subsequently taken after 24 h hydration in order to determine percent combined water. Differences in the rate of heat evolution and percent combined water were observed as a function of the glass content and the calcium aluminate type.

INTRODUCTION

It has long been known that the hydration of Portland cement proceeds exothermically [1,2]. Specific phases have been identified with certain thermo-evolution properties. The aluminate phase, C_3A ***, $C_{12}A_7$, etc., is known for its high heat generation and early hydration (setting) properties. The silicate phase, C_3S, C_2S, etc., is known for generating low heats of hydration and at a slower rate, in accordance with the slow hydration rates. Other thermo-events in the cement mixture are attributed to the formation of metastable species which act as necessary precursors to final hydration products.

---

* Now with Ciba-Geigy, Baton Rouge, LA, U.S.A.

** Author to whom correspondence should be addressed.

*** For brevity, cement chemistry notation is used throughout this paper: C = CaO, A = Al_2O_3, H = H_2O, M = MgO, $\bar{S} = SO_3$, S = SiO_2.

0040-6031/87/$03.50

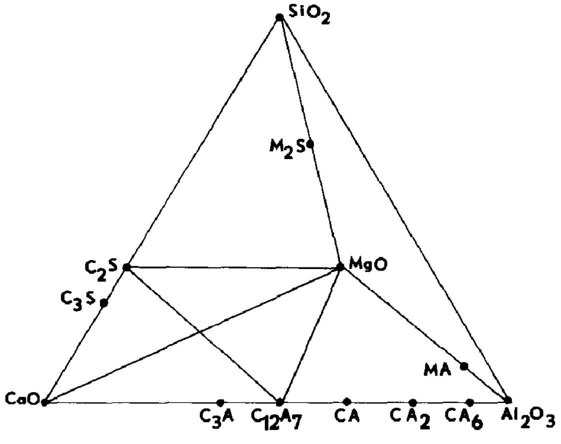

Fig. 1. Phase diagram for the system C–A–M–S.

The heat evolution has been attributed to various phenomena: heat of solution for the soluble compounds (C_3A, $C_{12}A_7$) and heat of crystallization of CH after reaching supersaturation followed by an induction period which precedes another thermo-event attributed to the formation of rigid gelatinous hydrated products of varying stoichiometries. Equations (1), (2), and (3) are examples of some of the reactions suggested [3].

$$C_6A_4MS + xH_2O = C_3AH_{8-12} + C_2AH_6 + \text{others} \qquad (1)$$

$$C_6A_4MS + xH_2O = C_3AH_6 + AH_3 + MH + CH + \text{others} \qquad (2)$$

$$3C_3A + xH_2O = C_2AH_8 + C_4AH_{19} + AH_3 + 3CH \qquad (3)$$

The rate of heat evolution and the total heat evolved over a period of time is of great interest to materials scientists and construction engineers in the cement industry. The information pertaining to the thermo-behavior could be used to design cementitious materials, either through synthesis or blending of materials from different batches. Thermo-histories could also be determined through heat evolution studies.

Previous studies were conducted on the synthesis and characterization of a series of aluminates. The quaternary phase diagram (Fig. 1) shows the studied phases. Hydration behavior of these compounds has been studied at various temperatures, namely 2, 25, and 50 °C at water to solid (W/S) ratios of 10 : 1, using an excess of water [3,4]. Heat evolution of the compounds reported here were conducted at 25 °C and W/S ratio of 0.5 over a 24-h period.

EXPERIMENTAL

The synthesis of high-purity calcium aluminates was described previously [4]. Table 1 lists some of the properties of the compounds studied. The

TABLE 1

Physical properties of the calcium aluminates

Compound	Surface area ($cm^2\ g^{-1}$)	Free lime (%)	Glass (%)
CA	2500	0.00	1.0
CA_2	2500	0.10	0.0
C_3A	2500	0.20	4.0
$C_{12}A_7$	2500	0.00	0.0
C_3A_2M (I)	2500	0.00	0.0
C_3A_2M (II)	2500	0.00	0.0
C_3A_2M (G)	2500	0.00	100.0
C_6A_4MS	2500	0.14	73.0

surface area was determined by the Blaine air permeability method, ASTM (American Society for Testing Materials) method C204-55. The free lime content was determined by the Franke method [5], solvent extraction of calcium oxide followed by acid titration. The last property listed in Table 1 is the percent glass content. This was determined by IR absorption spectroscopy [6] and petrography according to the "South African method" [7]. After synthesis, the materials were kept in glass vials and desiccated over ascarite and anhydrone before hydration.

A 1-g sample of the anhydrous material was introduced into a conduction calorimeter cell, described elsewhere [8], and allowed to equilibrate at 25°C in a water bath. After equilibration, 0.5 g of deionized distilled water at 25°C was injected into the calorimeter cell. The calorimeter cell was then vibrated for 5 s to facilitate homogeneous mixing. The hydration was allowed to proceed for 24 h. After 24 h the hydrated samples were removed from the cells, ground and washed in cold absolute methanol, followed by cold acetone in order to prevent further hydration. The samples were then dried at 105°C for 2 h in glass vials and vacuum desiccated over ascarite and anhydrone prior to thermogravimetric analysis (TGA).

Using a Mettler model TA-HE20 thermobalance, percent combined water was determined thermogravimetrically. Approximately 100 mg of sample were used per run. The TGA furnace was programmed for a maximum temperature of 1000°C at a rate of 10°C min^{-1} from 25°C, in a flowing air atmosphere.

RESULTS AND DISCUSSION

Some materials have significant initial (early) heat evolution preceded by an "induction" or dormant period which culminates into a large and prolonged exotherm (Fig. 2). The material C_3A_2M was prepared in three

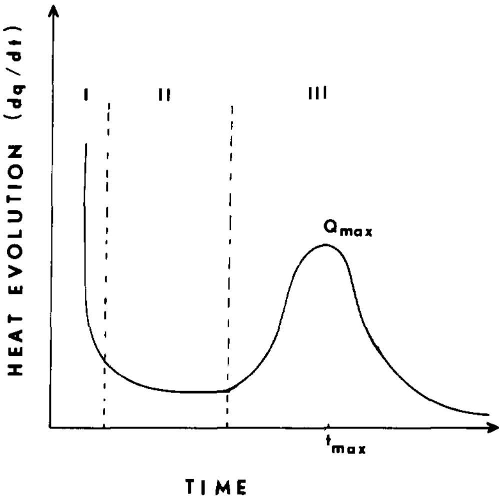

Fig. 2. Rate of heat evolution (dq/dt) vs. time profile showing an initial heat evolution stage (I), a dormant period (II), and a second heat evolution peak ending the dormant period.

forms. Two independently prepared samples were characterized as being 100% crystalline and a third sample was characterized as 100% glass [3]. Figure 3 depicts the heat evolution profiles of the three forms of these compounds. Warranting particular notice are the identical $t_{\max 1}$ and $t_{\max 2}$ values, for the two crystalline samples (I and II), and the shift in both $t_{\max 1}$ and $t_{\max 2}$ for the glassy material (G). The difference in the values of $Q_{\max}$

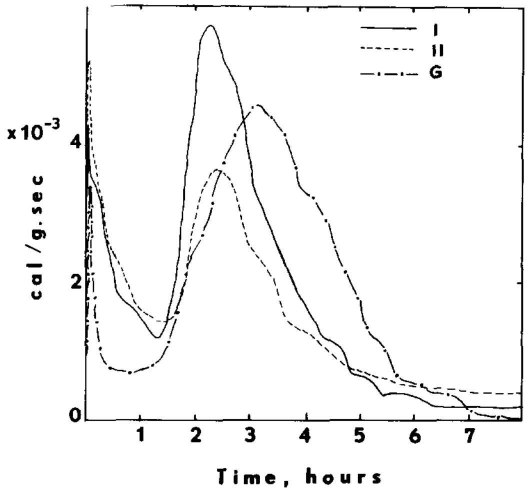

Fig. 3. Heat evolution rate curve for 100% crystalline C_3A_2M (I and II) and 100% glassy C_3A_2M (G). W/S = 0.5 at 25°C.

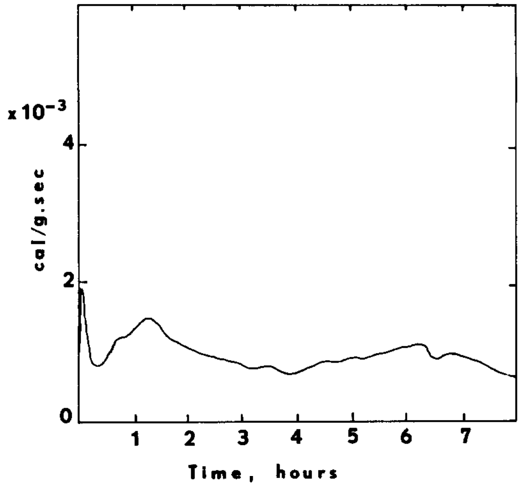

Fig. 4. Heat evolution rate curve for C_6A_4MS, 75% glass. W/S = 0.5 at 25°C.

for C_3A_2M (I) and C_3A_2M (II) is probably due to differences in particle size distributions. A high level of heat generation by the glassy material during the induction period is observed. The crystalline material does not generate as much heat during this period.

C_6A_4MS (Fig. 4) has an initial heat evolution peak and although it does not exhibit a large second Q_{max}, the system continues to generate a considerable amount of heat. This material was classified as being 73% glass [3]. Some compounds, such as C_3A characterized as 99% crystalline in this work, exhibit only one Q_{max} in a 24-h period (Fig. 5). No induction or dormant period follows; however, hydration product formation goes on well beyond 24 h. $C_{12}A_7$ (Fig. 6), which was synthesized in the crystalline form, has a thermo-behavior closely related to that of C_3A, but does, however, exhibit some peculiarities. It is an early hydrating species with t_{max} occurring 36 min after the t_{max} of C_3A. A shoulder is also observed right before t_{max} which could imply a latent dissolution–crystallization period. The heat curve does not drop to a $dq/dt = 0$, but remains at a plateau for 1 h. This is either delayed crystallization or rearrangement of metastable species. Powder XRD patterns did not show the presence of any impurities or other chemical species. Figure 7 shows the calorimetric output of the hydration of CA and CA_2. CA_2 does not hydrate exothermically or at least generate any detectable heat. CA exhibits exothermicity in the later stages of hydration, at about 10 h after mixing with water; no initial heat is recorded during the first hour. CA, therefore, has a dormant period that lasts about 6 h. The bimodal heat evolution profile of gypsum formation from a reagent grade hemihydrate (Fig. 8) shows the initial heat evolution within the first hour and a dormant period subsequent to Q_{max2}. The reagent grade hemihydrate was used as a standard for the calorimeter.

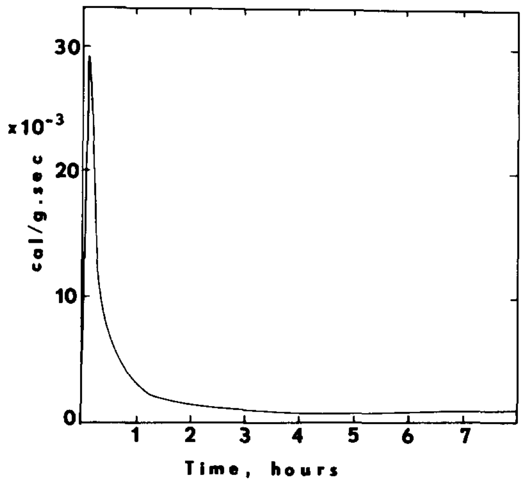

Fig. 5. Heat evolution rate curve for C_3A. W/S = 0.5 at 25 °C.

Several theories [2] have been proposed to try to explain the phenomena taking place in the three periods shown in Fig. 2. One prominent theory [9] advanced is that the first period, I, represents a period of rapid hydration, the second period, II, represents a period when hydrated species, i.e., eqns. (1), (2), and (3), are formed and the third period represents the precipitation or crystallization of portlandite (CH) which reaches supersaturation at the end of the induction period. Another theory [2,10] is that the first peak

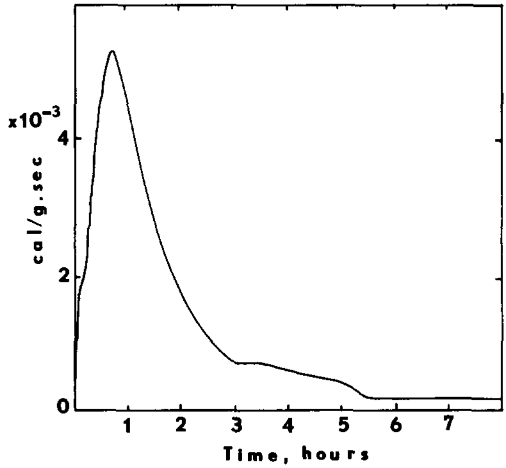

Fig. 6. Heat evolution rate curve for $C_{12}A_7$. W/S = 0.5 at 25 °C.

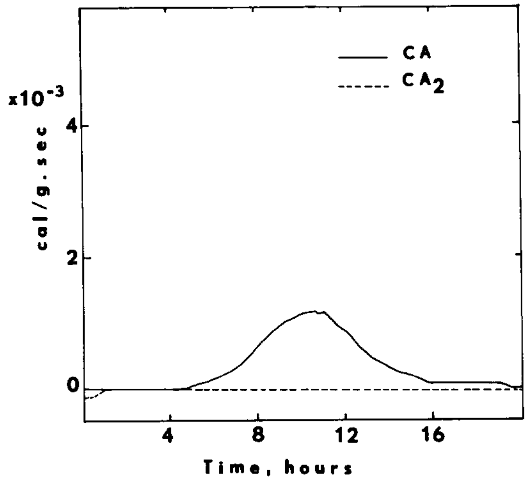

Fig. 7. Heat evolution rate curves for CA and CA_2. W/S = 0.5 at 25°C.

represents heat of solution or heat of wetting, in this case:

$$C_3A + xH_2O = Ca^{2+} + 2OH^- + C_nAH_y \tag{4}$$

$$Ca^{2+} + 2OH^- + C_nAH_y + xH_2O = C_2AH_8 + C_4AH_{19} + CH \tag{5}$$

and that this is especially so with moderately soluble materials. The second peak represents the heat of crystallization or hydrate formation, including formation of portlandite crystals. Materials with a high solubility, on the

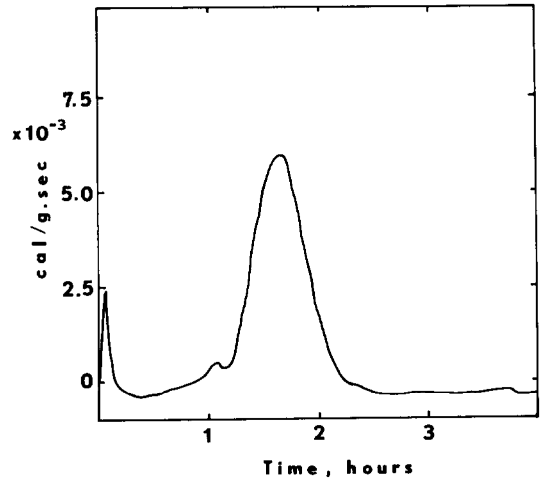

Fig. 8. The bimodal heat evolution rate curve for calcium sulfate hemihydrate ($C\bar{S}\cdot 1/2H$). W/S = 0.5 at 25°C.

TABLE 2

Maximum heat evolution rates and their corresponding t_{max} values

Compound	t_{max1} (min)	Q_{max1} (cal g^{-1} s^{-1}) $\times 10^{-3}$	t_{max2} (min)	Q_{max2} (cal g^{-1} s^{-1}) $\times 10^{-3}$
CA	–	–	666.00	1.14
CA_2	–	–	–	–
C_3A	6.00	30.34	–	–
$C_{12}A_7$	42.00	5.02	–	–
C_3A_2M (I)	3.00	4.93	148.00	3.41
C_3A_2M (II)	3.00	3.98	142.00	5.41
C_3A_2M (G)	2.00	2.75	190.00	3.60
$C_{\underline{6}}A_4MS$	4.00	1.95	–	–
$C\bar{S}\cdot 1/2H$	4.00	2.37	100.00	5.69

other hand, will tend to have only one peak (Q_{max1}), the initial peak. Likewise, materials on the other end of the solubility spectrum tend to have only one peak, the one that follows a long dormant period. Thus, CA would fall in this latter category, while C_3A and $C_{12}A_7$ fall in the former. For the latter category, the dormant period is said to be a period of formation of a semipermeable membrane around the solid particles which ruptures and releases heat, ending the induction period.

Thermogravimetric measurements of these compounds after 24 h hydration yielded results that showed no direct correlation of the t_{max} or the magnitude of Q_{max} (Table 2) and the percent combined water (Table 3). Previous studies [3,4] have shown, however, that early heat-evolving materials tend to achieve most of the hydration within the first 7 days of hydration after which the reaction rate decreases significantly. This rate decrease affects the strength-developing behavior of the materials. The absence of further and continued hydration results in a material of reduced strength. Those compounds whose Q_{max} occurs late tend to continue hydrating at a steady rate, thus contributing to the strength of the material.

TABLE 3

TGA results after 24 h hydration

Compound	% combined H_2O	Compound	% combined H_2O
CA	18.90	C_3A_2M (II)	31.20
CA_2	14.50	C_3A_2M (G)	36.30
C_3A	31.50	$C_{\underline{6}}A_4MS$	36.60
$C_{12}A_7$	26.54	$C\bar{S}\cdot 1/2H$	5.08
C_3A_2M (I)	32.10		

CONCLUSION

Several factors affect the hydration behavior of cementitious materials: namely, W/S ratio, particle size, pore size and pore size distribution, glass content, humidity, pressure, and temperature [2,3,11]. Earlier work demonstrates that low temperatures seem to promote hydration of C_3A [3]. Hydration of the silicates, on the other hand, is facilitated by high temperatures. It must be this synergism that makes Portland cement such a practical and versatile construction material. The heat generated by the early setting compounds is absorbed and used to facilitate hydration of the slow hydrating materials.

In this work, various modes of heat evolution have been reported. No direct relationship was found between heat evolution rate maximum, Q_{max}, and percent combined water for a 24-h period. The area under the curve which represents the total heat generated may have a relationship with the percent combined water. In general, materials that generate heat during the early stages of the hydration reaction process will have a high yield of hydration products or will hydrate faster in the first 24 h of hydration. For C_3A_2M, the crystalline material generates heat longer (i.e. $dq/dt > 0$) during the dormant period, while the highly glassy materials approach zero heat evolution rate ($dq/dt = 0$) during the same period.

ACKNOWLEDGMENTS

Financial support from the R.A. Welch Foundation and the Gillette Co. is gratefully acknowledged. The TGA analyses were performed by Mr. Jin-Mo Huang of North Texas State University, Denton, TX, U.S.A.

REFERENCES

1 R.H. Bogue, The Chemistry of Portland Cement, Reinhold, New York, 1947, pp. 79–85.
2 R. Kondo and S. Ueda, Proc. 5th. Int. Symp. on the Chemistry of Cement, Vol. 2, Tokyo, 1968, pp. 203–248.
3 J.G. Griffin, Ph.D. Dissertation, North Texas State University, Denton, TX, 1984.
4 J.G. Griffin and K.E. Daugherty, Thermochim. Acta, 91 (1985) 53.
5 ASTM Designation: C204-55, ASTM Book of Standards, Part IV, 1958, pp. 140–146.
6 A.R. Eberendu and K.E. Daugherty, Cem. Concr. Res., 14 (1984) 873.
7 F.R. Fulton, Portland Cement Institute Monograph, Johannesburg, 1974, pp. 6, 7.
8 T.P. Zgambo, M.D. Cohen and K.E. Daugherty, Thermochim. Acta, 108 (1986) 79.
9 M.E. Tadros, J. Skalny and R.S. Kalyocu, J. Am. Ceram. Soc., 59 (1976) 344.
10 S. Goto, M. Daimon, G. Hosaka and R. Kondo, J. Am. Ceram. Soc., 59 (1976) 281
11 K.E. Daugherty, B. Saad, C. Weirich and A.R. Eberendu, Silic. Ind., 48 (1983) 107.